Desalination and Water Treatment
www.deswater.com

doi: 10.5004/dwt.2018.22481

121 (2018) 219–232
July

Biosorption and kinetic studies of Malachite Green (MG) dye removal from aqueous solution using a low-cost adsorbent prepared from male palm tree flower (*Borassus flabellifer*)

A. Babu Ponnusami*, Sathish Kumar, Prayag Bansal

Department of Chemical Engineering, VIT University, Vellore, Tamilnadu, India, Tel. +91 9443691869; email: ababuponnusami@vit.ac.in (A. Babu Ponnusami)

Received 19 March 2018; Accepted 8 May 2018

ABSTRACT

Activated carbon derived from male palm tree flower (MPTF) (*Borassus flabellifer*) was used as adsorbent to adsorb Malachite Green (MG) dye. Batch adsorption studies were performed by varying the parameters like initial solution pH, adsorbent dosage, initial dye concentration and temperature with activated carbon prepared from MPTF. The maximum dye removal (>95%) was occurred at an optimum pH of 6.0, and zero point charge was found to be 2.75. Isotherm models such as Langmuir, Freundlich, and Temkin were used to analyse the experimental data, and it was found that the Langmuir isotherm model was best fitted with the adsorption data. Further, the separation factor (R_L) value was less than unity indicating a favourable adsorption process. Thermodynamic parameters such as ΔG, ΔH, and ΔS were calculated for the adsorption processes and indicate that the adsorption process was spontaneous and endothermic in nature. Adsorption rate constants were determined using pseudo-first-order, pseudo-second-order rate equations, and also Elovich model and intraparticle diffusion models. The results clearly showed that the adsorption of MG followed pseudo-second-order model, and the adsorption was controlled by intraparticle diffusion.

Keywords: Malachite Green; Adsorption isotherm; Kinetics; Thermodynamic; Male palm tree flower

1. Introduction

Industrialisation and urbanisation in recent decades create more complex problems on environment [1,2]. Textile industries were grown tremendously in recent years and discharges unprecedented amount of wastewater containing synthetic dyes. This wastewater pollutes the environment and causes harmful effects on human and other living organisms [3]. Due to the carcinogenic and mutagenic effects of synthetic dye, aquatic life and food webs are readily affected, and the aesthetic and keeping quality of water is reduced [4,5].

Textile industries require large quantity of reactive dyes due to increasing utilisation of cellulosic fibres. This is due to the technical advancement and higher cost of other dyes used for these fibres [6,7].

Synthetic dyes are having good solubility in nature and commonly found in textile, leather, and paper industries. Around 2% of dyes produced annually are wasted in effluent from manufacturing operations [8].

The complex aromatic structure and strong physicochemical, thermal, and optical stability of synthetic dyes makes the biodegradation process as more difficult [9]. Hence, suitable treatment method should be devised. In recent years, many methods such as coagulation and flocculation [10], chemical oxidation [11,12], bio-based treatments [13,14], reverse osmosis [15], photooxidation [16], and physical adsorption [17,18] have been developed for treating textile wastewater.

* Corresponding author.

Presented at the 3rd International Conference on Recent Advancements in Chemical, Environmental and Energy Engineering, 15–16 February, Chennai, India, 2018.

Literature study indicates that the adsorption process was one of the most efficient techniques for dye removal. It is likely due to its simplicity and high level of usefulness as well as the availability of a wide range of natural and synthetic adsorbents. Among the adsorbents present, activated carbon is the most popular adsorbent for removal of dyestuffs from wastewater [5]. However, making activated carbon with high adsorption capacity is cost prohibitive and has regeneration and disposal problems. Therefore, there is a growing demand for freely and locally available low-cost natural materials for the removal of dyes.

In recent years, various natural materials such as rice husk [9], pyrophyllite [19], coir pith [20], montmorillonite [21], fungi [22], soil [23], clay mineral [24,25], bagasse [26], tamarind fruit shell [27], water hyacinth root [28], *Cucumis sativa* fruit peel [29], rubber seed coat [30], water nut carbon [31], *Borassus aethiopum* flower [32], and materials from agricultural wastes [33–35] have been used and investigated for removal of various dyes from aqueous solution.

This paper focused on the evaluation of adsorption potential of the activated carbon prepared from male palm tree flower (MPTF) for the treatment of synthetics wastewater containing Malachite Green (MG). MPTF is freely and abundantly available villages. Batch studies were carried out to find the adsorption potential of MPTF by considering the influencing parameters such as initial dye concentration, adsorbent dose, pH, and temperature. The experimental data were taken for adsorption kinetics and thermodynamic analysis. Also the adsorption mechanism was understood by fitting the experimental data with various isotherm models, and the performance of newly developed adsorbent was compared with the other adsorbent for the removal of MG from aqueous solution.

2. Materials and methods

2.1. Adsorbate

Commercial grade MG (CAS no. 569-64-2) is a cationic dye with a molecular formula $C_{23}H_{25}ClN_2$ and molecular weight of 364.911 g/mol purchased from Merck (Mumbai, India) and used without further purification. The maximum absorption wavelength of this dye is 618 nm. The structure of MG is shown in Fig. 1.

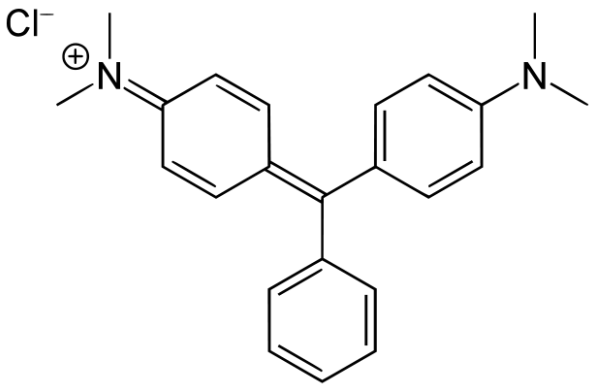

Fig. 1. Structure of Malachite Green.

2.2. Preparation of biosorbent

MPTFs collected from villages near by Tiruvannamalai, India, were washed thoroughly with distilled water to remove dirt particles and water soluble particles adhered to the surfaces. The flower was cut into small pieces and dried in oven at 70°C for 1 d. Then the carbonisation of particle was carried out at 300°C for 24 h in muffle furnace. The particles were further ground into powder by using ball mill and sieved to obtain average particle size of 150 μm. The powdered particle was stored in an airtight container for further use. No other chemical treatments were used prior to adsorption experiments.

2.3. Characterisation of MPTF

The adsorbent, MPTF, was characterised with Fourier-transform infrared (FTIR) spectroscope (FT-IR-2000, PerkinElmer, Chennai, India) and was used to find the surface functional groups of MPTF. In this analysis, aliquots of the sample were diluted and mixed with KBr to produce KBr pellets and then vacuum pressed. Absorbance spectra were recorded from 4,000 to 400 cm^{-1} with 16 cm^{-1} resolution. Surface morphology of MPTF powder was studied using scanning electron microscopy (SEM) (VEGA3 TESCAN) image.

The zero point charge of MPTF was determined by suspending 1.0 g of the MPTF in 1 m mol/L of NaCl solution for 36 h. A total of 60 ml of the suspension was taken into eight conical flasks, and the initial pH was adjusted to 2.05, 3.16, 4.15, 5.18, 6.24, 7.26, 8.28, and 9.32. The suspensions were allowed to reach equilibrium, and the final pH of the samples was measured. The results were plotted as ΔpH against initial pHi.

2.4. Biosorption experiment

2.4.1. Effect of pH

The effect of pH on amount of colour removal was analysed over a pH range of 2–10. NaOH (0.1N) and H_2SO_4 (0.1N) solutions were used to adjust pH. In this study, experiments were carried out in 1,000 mL of dye solution with 100 mg/L of initial dye concentration, 2 g/L of MPTF powder at room temperature of 30°C. Agitation was carried out for 1.5 h which is more than sufficient to reach equilibrium at constant agitation of 200 rpm. The aliquots samples were withdrawn at regular time interval and centrifuged immediately to separate adsorbent particles. Remaining dye concentrations in samples were determined by measuring the absorbance at the characteristics wavelength of MG (λ_{max} = 618 nm) using UV-vis spectrophotometer (Systronics, Ahmedabad, India).

2.4.2. Biosorbent dosage

Adsorption efficiency depends on biosorbent dosage. Hence, adsorbent amount was varied from 0.5 to 3 g/L to find the effect of dosage by maintaining initial concentration of dye as 100 mg/L. All the experiments were carried out at 30°C, pH of 6, and 200 rpm for 90 min.

2.4.3. Biosorption equilibrium study

The equilibrium studies were carried out at 200 rpm by adding 2 g/L of MPTF to 1,000 ml of dye solution. The dye

concentration was varied from 50 to 300 mg/L, and all the experiments were performed in triplicates. The amount of MG adsorbed per gram of MPTF (q_e) was obtained using the following expression:

$$q_e = \frac{(C_i - C_e)V}{M} \quad (1)$$

where C_i and C_e are the initial and equilibrium concentrations (mg/L) of dye, respectively; q_e is the equilibrium uptake value (mg/g), V is the volume of the solution (L), and M is the dry weight of the adsorbent (g). The percentage removal of the dye is given by the following equation:

$$\% \text{ Removal} = \frac{(C_i - C_e)}{C_i} \times 100 \quad (2)$$

2.4.4. Effect of temperature

For thermodynamic study, the experiments were performed by varying temperature from 30°C to 60°C (30°C, 40°C, 50°C, and 60°C) at a constant pH of 6. For these experiments, 2 g/L of MPTF added to 1,000 ml of dye solution in 1.5 L flasks. The flasks were shaken at 200 rpm for 180 min. The initial dye concentration used in this study was 50–300 mg/L. After agitation, the reduction in dye concentration was measured at regular time intervals. All experiments were carried out in triplicate under identical conditions and mean values are presented.

3. Results and discussion

3.1. Characterisation of biosorbent

FTIR spectroscopic analysis was studied to find the surface functional groups on sorbent, and results are shown in Figs. 2(a) and 2(b). The characteristic peaks correspond to 3,277 cm^{-1} represent –OH group of lignin, and the presence of $–CH_2$ group is confirmed with the band about 2,920 cm^{-1} [36,37].The band observed at 1,726 cm^{-1} confirms the C=O stretching of aldehyde [38], while the peak at 1,606 cm^{-1} was attributed to C=C stretching of phenol group [39]. The aromatic ring of lignin was confirmed with stretching at 1,440 cm^{-1}, and the band in 1,249 cm^{-1} confirms the bending mode of C–C–H, C–O–H, and O–C–H. The presence of C–O bond was confirmed with the band at 1,029 cm^{-1} which confirm the presence of lignin in MPTF [39].

The spectral analysis of the MPTF-activated carbon powder before and after adsorption (Figs. 2(a) and 2(b)) process confirms that the –OH group and other groups are responsible for the adsorption of MG.

The surface morphological changes of adsorbent before and after the desired process were observed using SEM (VEGA3 TESCAN), and images are shown in Figs. 3(a) and 3(b). From the figures, it is observed that the surface of the sorbent before use contains rough and irregular layers that will enable sorption. The micropores in sorbent are responsible for adsorption and adsorb the dye molecules more readily. Also from Fig. 3(b), it was observed that the surface of the sorbent was completely covered by thick layer of adsorbate, and the micropores present on the surface before adsorption were not seen because the micropores were occupied by sorbate molecules.

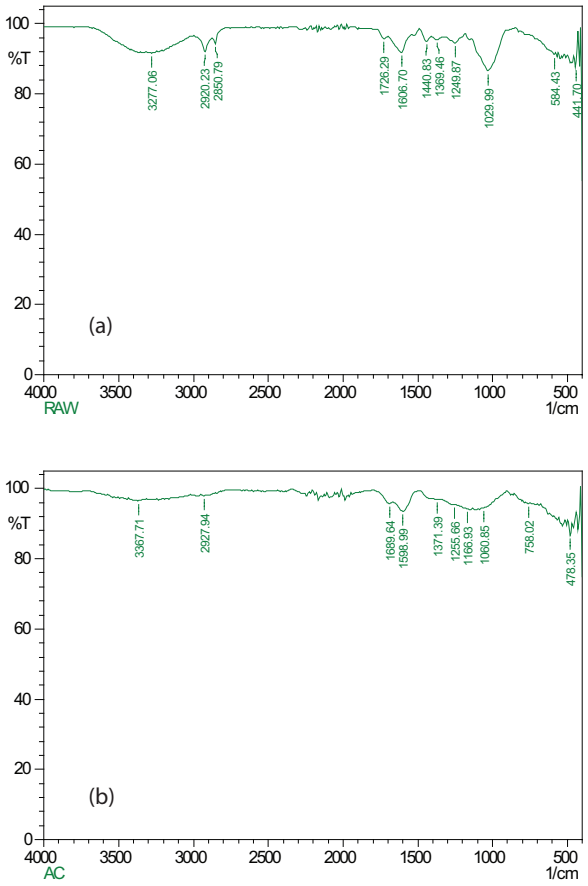

Fig. 2. FTIR spectra of MPTF carbon powder: (a) before adsorption and (b) after adsorption.

3.2. Effect of solution pH

The pH of solution plays an important role on adsorption capacity, where it affects both surface properties of biosorbent as well as degree of ionisation. Experiments were performed at pH range of 2.0 to 10.0, and the results are shown in Fig. 4. From the results, it was observed that the removal of dye increases with increase in pH from 2.0 to 6.0. Further increase in pH did not favour dye adsorption, instead the percentage adsorption was decreased from 96.4% to 75.23%. This could be due to the adsorption of OH^- ions and negatively charged surface at higher pH values and was confirmed with point zero charge of adsorbent. The point zero charge of PTMF was found to be 2.75 (figure not shown). At very low pH ($pH < pH_{pzc}$), H^+ ions that are adsorbed on the PTMF surface may get positively charged. Due to this adsorption, a repulsive force occurs between the cation dye molecules and the biosorbent surface. This leads to lowering of the adsorption capacity at low pH, and similar trends were reported in literature [40].

The increase in solution pH above pH_{pzc}, will favour the adsorption, and the percentage dye removal increased continuously as long as the dye molecules are still positively charged or neutral even though the MPTF surface is negatively charged due to adsorption of OH^- ions. When the surface charges of adsorbent and dye molecules are negative, then the percentage dye removal decreases. The maximum adsorption was obtained at a pH of 6. Further increase in pH did not favour the adsorption process. Therefore, pH 6 was used for further adsorption studies. Similar trends were observed by various authors for MG adsorption on rice bran [41], bivalve shell [42], and rubber seed coat [43].

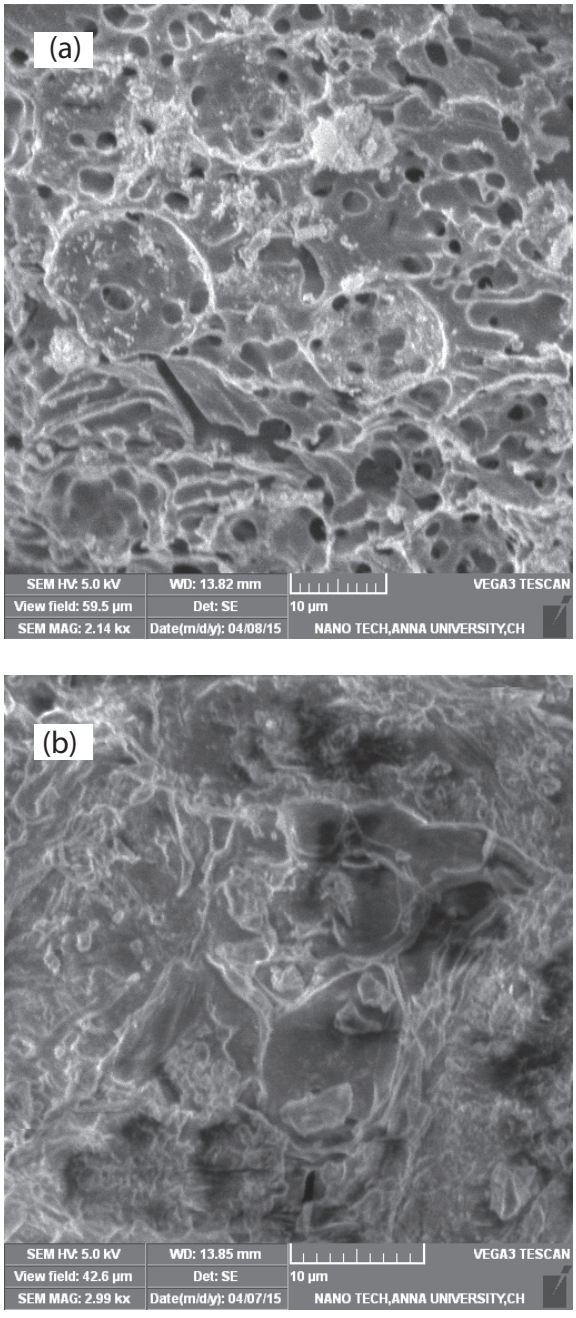

Fig. 3. SEM images of MPTF powder: (a) before adsorption and (b) after adsorption process.

3.3. Effect of adsorbent dose

The effect of adsorbent dosage on both percentage dye removal and the amount of dye adsorbed per unit weight of adsorbent is shown in the Fig. 5. From the figure, it is clearly observed that the percentage removal of dye is directly proportional to the adsorbent dosage to a certain extent and then it remains almost constant. The sorption rate increased from 58.2% to 92.6% at equilibrium as MPTF dose was increased from 0.5 to 3 g/L, and optimum dosage was found to be 2 g of MPTF per litre of dye solution. This may be due to the increase in surface area of the adsorbent and availability of more adsorption sites [5]. However, capacity of adsorbent toward dye removal was decreased with increase in biosorbent dosage. It decreased from 116.4 to 31.7 mg/g as the biosorbent dose increased from 0.5 to 3 g/L. This may be due to the following reason: sorption sites are overlapped one another above as a result biosorbent particles are overcrowded, and similar results were found in literature [44,45].

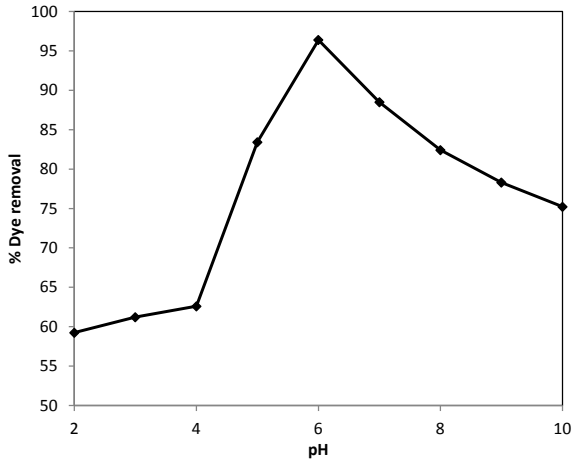

Fig. 4. Effect of pH on dye removal (condition: initial dye concentration = 100 mg/L, MPTF powder = 2 g/L, adsorbent size = 150 µm, contact time = 90 min).

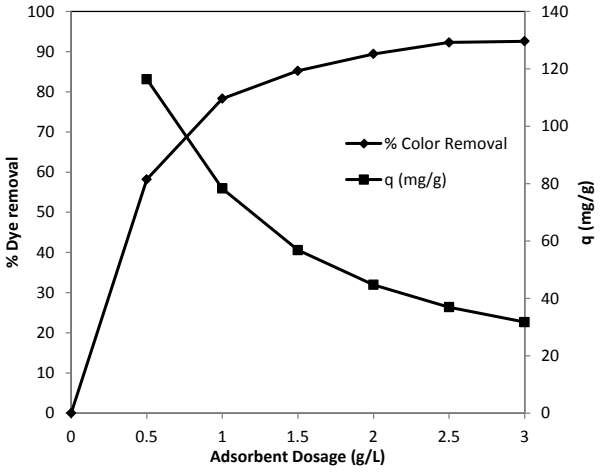

Fig. 5. Effect of MPTF dosage on dye removal (condition: initial dye concentration = 100 mg/L, pH = 6.0, adsorbent size = 150 µm, contact time = 90 min).

3.4. Effect of temperature

Experiments were performed at different temperatures of 30°C, 40°C, 50°C, and 60°C for the initial MG concentrations of 50–300 mg/L at constant adsorbent dose of 2 g/L. The percentage adsorption increased from 87.2% to 97.2%, 78.8% to 89.8%, 62.0% to 71.5%, 49.72% to 57.22%, 38.4% to 45.2%, and 30.5% to 35.5% for the initial MG concentrations of 50, 100, 150, 200, 250, and 300 mg/L, respectively with increase in temperature from 30°C to 60°C (Fig. 6). This behaviour of adsorption indicates that the process of MG dye removal is an endothermic process. This may be due to the higher mobility of dye molecules at high temperature and increase in the number of active sites for adsorption and also due to the enlargement of pore size and activation of adsorbent surface [46].

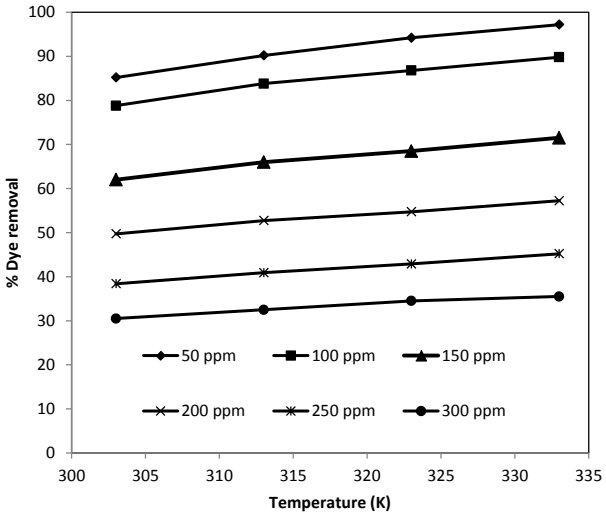

Fig. 6. Effect of temperature on dye removal (condition: initial dye concentration = 50–300 mg/L, pH = 6.0, MPTF = 2 g/L, size of adsorbent = 150 μm, and contact time = 90 min).

3.5. Biosorption equilibrium study

The relationship between the adsorbate in the liquid phase and solid phase at equilibrium and at constant temperature is called adsorption isotherm. The equilibrium adsorption isotherm is very important to design the adsorption systems, and it plays an important role to find the maximum capacity of adsorption [5]. It also provides the knowledge about how efficiently and economically an adsorbent used in the system. In order to study the effect of temperature on the equilibrium capacity of MPTF and an adequate model that can reproduce the experimental results obtained, Langmuir, Freundlich, and Temkin isotherms have been considered.

3.5.1. The Langmuir isotherm

The theoretical Langmuir isotherm equation was developed based on the assumptions such as all the specific homogeneous sites were occupied with adsorbate and no further adsorption at equilibrium. The maximum adsorption occurs under the following conditions: when the adsorbent surface was filled with a saturated monolayer of solute molecules, the energy of adsorption is constant, and there is no migration of adsorbate molecules in the surface plane. The nonlinear form of Langmuir isotherm model was expressed as follows [47]:

$$q_e = \frac{q_m K_L C_e}{1 + K_L C_e} \quad \text{(or)} \quad \frac{C_e}{q_e} = \frac{1}{q_m K_L} + \frac{C_e}{q_m} \tag{3}$$

where C_e is the supernatant concentration at the equilibrium state of the system (mg/L), q_e is the amount adsorbed (mg/g), and q_m and K_L are the Langmuir constants representing the maximum adsorption monolayer capacity (mg/g) for the solid phase loading and the energy of adsorption (L/mg), respectively. These constants can be determined from the linear plot of C_e/q_e vs. C_e (Fig. 7) and shown in Table 1 together with R^2 values.

The measure of goodness-of-fit for any experimental data is represented by correlation coefficient (R^2) values. From Table 1, it is observed that the R^2 values for Langmuir isotherm were all higher than 0.99, indicating a very good mathematical fit. Also, it may be predicted from Table 1 that the increase of monolayer adsorption capacity (q_m) with increase in temperature indicates adsorption of MG on MPTF is an endothermic process. Similar results are observed in literature [46].

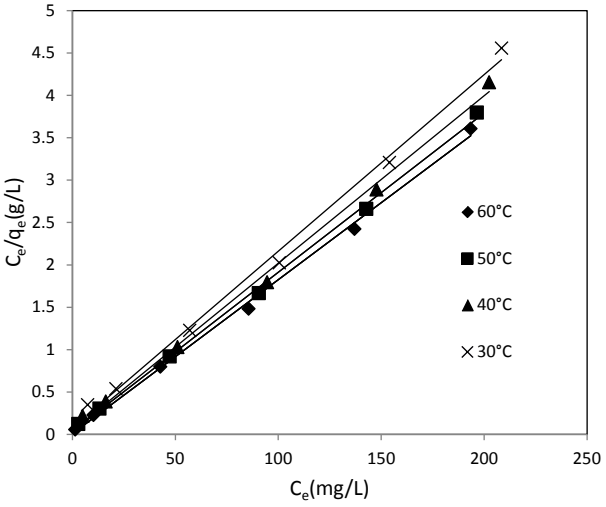

Fig. 7. Langmuir isotherm for dye removal at various solution temperatures using ESP (condition: pH = 6.0, dosage of MPTF = 2 g/L, size of adsorbent = 150 μm, and contact time = 180 min).

The affinity between the adsorbate and adsorbent can be predicted using the separation factor or dimensionless equilibrium parameter 'R_L', which is a function of Langmuir isotherm parameter and is expressed as in the following equation [48]:

$$R_L = \frac{1}{1 + K_L C_0} \tag{4}$$

where K_L is the Langmuir constant and C_0 is the initial concentration of MG. The values of separation factor R_L provides important information about the nature of adsorption. It indicates the type of isotherm to be irreversible (R_L = 0),

Table 1
Equilibrium parameters of Langmuir, Freundlich, and Temkin constants for the adsorption of dye on MPTF

Solution temperature (°C)	Equilibrium isotherm								
	Langmuir constant			Freundlich constant			Temkin constant		
	q_m (mg/g)	K_L (L/mg)	R^2	K_f (mg/g)	n	R^2	A (L/mg)	B	R^2
30	48.07	0.266	0.9954	16.71	4.57	0.7528	5.20	7.376	0.784
40	50.51	0.4620	0.9968	19.88	5.04	0.7662	10.965	7.1023	0.799
50	53.19	0.5513	0.9986	22.71	5.49	0.822	21.93	6.817	0.856
60	54.95	2.395	0.9978	26.23	6.1	0.8563	60.53	6.366	0.885

Table 2
Effects of initial dye concentrations on dimensionless separation factor (R_L) at different solution temperatures

Initial dye concentration (mg/L)	Values of R_L at different temperatures			
	30°C	40°C	50°C	60°C
50	0.06993	0.04149	0.03501	0.00828
100	0.03623	0.02119	0.01782	0.00416
150	0.02445	0.01422	0.01195	0.00278
200	0.01845	0.01071	0.00899	0.00208
250	0.01481	0.00858	0.00720	0.00167
300	0.01238	0.00716	0.00601	0.00139

favourable ($0 < R_L < 1$), and linear ($R_L = 1$) or unfavourable ($R_L > 1$) [49,50]. The values of R_L for the sorption of MG dye on the MPTF powder are shown in Table 2. From the table, it was observed that the values of R_L are less than one and greater than zero that supports previous observation where the Langmuir isotherm was favourable for the dye sorption at all studied temperatures [45].

3.5.2. The Freundlich isotherm

The Freundlich isotherm model is the earliest known relationship describing the adsorption process. This model is based on the mechanism of adsorption on heterogeneous surfaces and also suggests that sorption energy exponentially decreases on completion of the process. Empirical equation of Freundlich isotherm is expressed as follows:

$$q_e = K_f C_e^{\frac{1}{n}} \quad \text{(or)} \quad \log q_e = \log K_f + \frac{1}{n}\log C_e \tag{5}$$

where K_f is the Freundlich constant (L/g) related to the bonding energy. K_f can be defined as the adsorption or distribution coefficient and represents the quantity of dye adsorbed onto adsorbent for unit equilibrium concentration. The measure of deviation from linearity of adsorption is given by n. The adsorption process is classified according to the range of 'n' values such as linear adsorption ($n = 1$), chemisorption ($n < 1$), and physical sorption ($n > 1$) [51]. The experimental data were fitted with Freundlich equation (Fig. 8), and the constant from the graph are shown in Table 1.

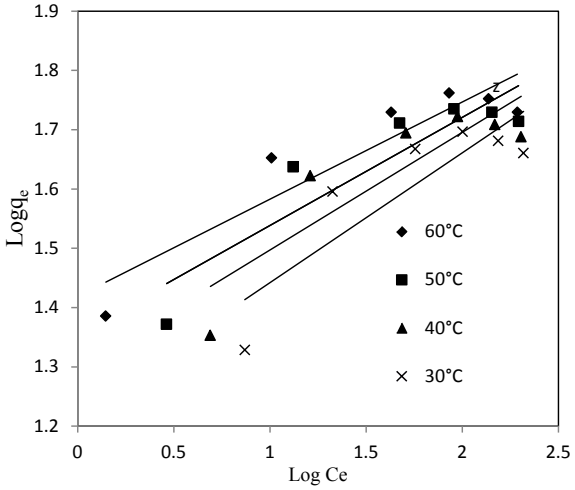

Fig. 8. Freundlich isotherm for dye removal at various solution temperatures using MPTF (condition: pH = 6.0, dosage of MPTF = 2 g/L, size of adsorbent = 150 μm, and contact time = 180 min).

From the table, it was observed that the value of n was found to be in the range of 4.57–6.1. This indicates that the present adsorption process was physical process. Similar results were observed in previous literatures [52–54]. From Fig. 8, it is observed that a linear relation was observed among the parameters at different temperatures. However, on comparison of regression coefficients (R^2) for both Langmuir and Freundlich isotherms, it is confirmed that the equilibrium data are well fitted with the Langmuir isotherm for the different temperatures studied.

The predicted Langmuir and Freundlich isotherm constants at 30°C for MG dye on to MPTF are useful for design calculations and is given by Eqs. (6) and (7), respectively.

$$q_e = \frac{12.835 C_e}{1 + 0.266 C_e} \tag{6}$$

$$q_e = 16.71 C_e^{0.219} \tag{7}$$

The nonlinear plots generated from Langmuir and Freundlich isotherm at 30°C using Eqs. (6) and (7) are shown in Fig. 9. From the figure, it was observed that the experimental data are well fitted with the Langmuir isotherm

equation when compared with the Freundlich isotherm equation, which confirms the monolayer adsorption of the dye onto the MPTF [55].

3.5.3. Temkin isotherm

The interaction between adsorbate and adsorbent can be studied well by Temkin isotherm [56,57]. This model was developed by assuming following: (i) due to the adsorbent–adsorbate molecule interactions, the heat of adsorption decreases linearly and that (ii) uniform distribution of binding energies between adsorbent and adsorbate molecules characterise the adsorption process. Temkin isotherm is commonly written as follows:

$$q_e = B\ln\left(AC_e\right) \quad (\text{or}) \quad q_e = B\ln\left(A\right) + B\ln\left(C_e\right) \tag{8}$$

where A and B are Temkin isotherm constants. The Temkin constant B represents the heat of adsorption, and A represents equilibrium constant at maximum binding energy. Constants A and B are calculated from the linear plot between q_e vs. $\ln C_e$ (Fig. 10), and the values are shown in Table 1. From the table, it may be concluded that the constant representing heat of adsorption decreases and the constant representing binding energy increases as the solution temperature increases.

3.6. Adsorption kinetics studies

The effectiveness of an adsorbent depends upon the residence time of adsorbent, and kinetics studies guide the rates that determine the residence time. The kinetic profiles of MG biosorption onto MPTF were investigated in this section.

3.6.1. Effect of contact time

Fig. 11 shows the effect of contact time on removal rate of MG by powdered MPTF. Experimental studies were carried out with varying initial dye concentrations ranging from 50 to 300 mg/L using 2 g/L of adsorbent dose at pH 6. From the figure, it was observed that the percentage dye removal was increased proportionally with the agitation time and reached equilibrium after 90 min for the dye concentrations used in this study. This time is known as equilibrium time, and adsorption capacity of adsorbent is reflected by equilibrium time [58].

The percentage removal of MG at equilibrium was decreased from 96.4% to 33.2% as the dye concentration increased from 50 to 300 mg/L. This may be due to the following reason that increase in initial dye concentration provides driving force to overcome all resistances of the dye between the aqueous and solid phases [45,59]. At lower concentrations, all sorbate ions present in the sorption medium could interact with the binding sites, hence higher percentage removal was obtained. At higher concentrations, the percentage removal of the dye shows a decreasing trend due to the saturation of the sorption sites [45,55].

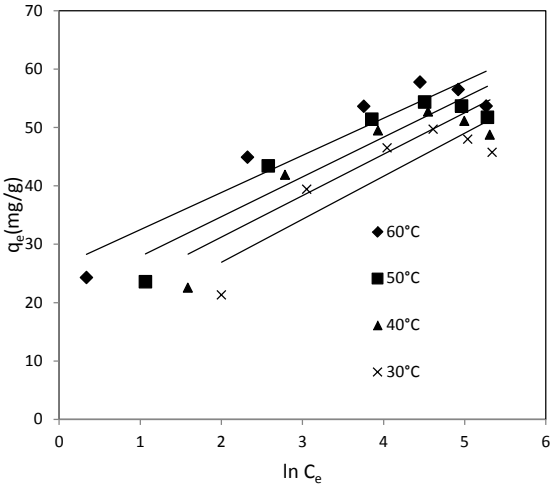

Fig. 10. Temkin isotherm for dye removal at various solution temperatures using MPTF (condition: pH = 6.0, dosage of MPTF = 2 g/L, size of adsorbent = 150 μm, and contact time = 180 min).

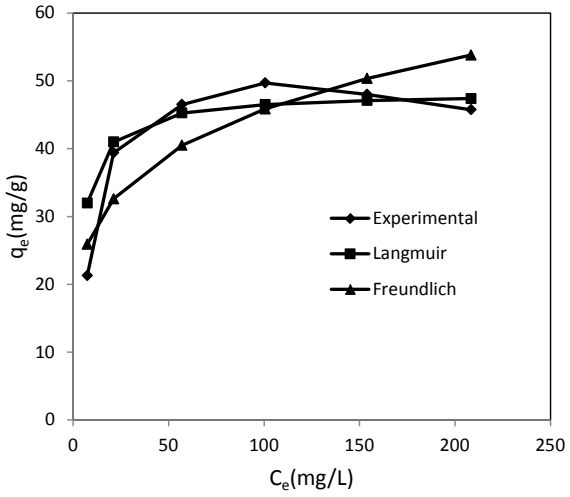

Fig. 9. Nonlinear equilibrium plots for dye removal at 30°C using the MPTF (condition: pH = 6.0, dosage of MPTF = 2 g/L, size of adsorbent = 150 μm, and contact time = 180 min).

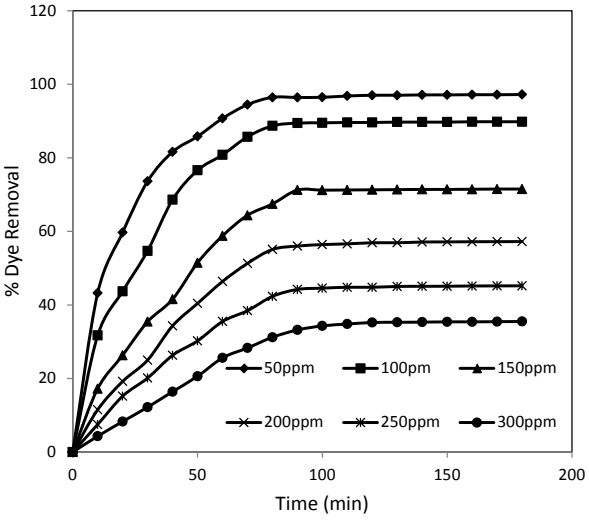

Fig. 11. Effect of contact time on percentage dye removal (condition: pH = 6.0, dosage of MPTF = 2 g/L, size of adsorbent = 150 μm, and temperature = 30°C).

3.6.2. Effect of initial dye concentration

Adsorption of MG onto MPTF was studied at different initial dye concentration (50–300 mg/L) at sorbent dosage of 2 mg/L. The comparison between percentage dye removal and sorbent uptake capacity at equilibrium time are shown in Fig. 12. From the figure, it is evident that the amount of dye adsorbed at equilibrium increases from 24.1 to 56 mg/g for an increase in initial dye concentration from 50 to 200 mg/L.

A higher uptake capacity at higher concentration is due to the availability of more driving force to overcome all resistances. But, further increase in initial dye concentration to 250 and 300 mg/L did not favour to increase in uptake capacity; instead the uptake capacity decreases to 55.25 and 49.8 mg/L, respectively [55]. This is due to the saturation of sorption sites by dye molecules at higher concentration. On the other hand, the percentage dye removal shows a decreasing trend as the initial dye concentration increases. At lower dye concentrations, all adsorbate ions present in the medium could interact with the binding sites, hence percentage removal was higher. At higher dye concentrations, because of quick saturation of the sorption sites, the percentage dye removal shows a decreasing trend [55]. Similar trend was observed by the other investigators [60,61].

3.6.3. Adsorption kinetic modelling

In order to investigate the mechanism of adsorption and steps that govern the overall removal rate in the adsorption process, kinetic models have been used. The pseudo-first-order, pseudo-second-order, Elovich, and intraparticle diffusion were tested to fit the experimental data obtained for MG uptake by MPTF. The rate constant and equilibrium uptake values for the adsorption process were determined using the model equations.

Chi square and the normalised standard deviation given by Eqs. (5) and (6) were used to validate the kinetics models [62].

$$\psi^2 = \frac{\left(q_{\exp} - q_{\text{cal}}\right)^2}{q_{\text{cal}}} \tag{9}$$

$$\Delta q_e(\%) = 100\sqrt{\left|\frac{(q_{\exp} - q_{\text{cal}})/q_{\exp}}{N-1}\right|} \tag{10}$$

where N is the number of data points while $q_{\exp}$ and q_{cal} are experimentally determined quantity adsorbed at equilibrium and calculated quantity adsorbed at equilibrium, respectively.

3.6.3.1. The pseudo-first-order model The pseudo-first-order kinetic model with respect to solid/liquid adsorption system can be written as follows [63]:

$$\ln\left(q_e - q_t\right) = \ln q_e - k_1 t \tag{11}$$

where q_e (mg/g) refers to the amount of dye adsorbed at equilibrium, q_t (mg/g) refers to amount of dye adsorbed at time 't', and k_1 is rate constant for pseudo-first-order adsorption. The value of pseudo-first-order rate constant, k_1, has been evaluated from the slope of the linear plot of $\ln(q_e - q_t)$ vs. t as shown in Fig. 13. The values of k_1 and q_e calculated from the model equation and correlation coefficient (R^2) values at different dye concentrations are presented in Table 3.

The linear plot of first-order model (Fig. 13) recommended that the process of dye adsorption did not follow the first-order rate kinetics. This can be confirmed from the chi square and Δq_e(%) values shown in Table 3. These values are higher than the other models for the studied dye concentration range.

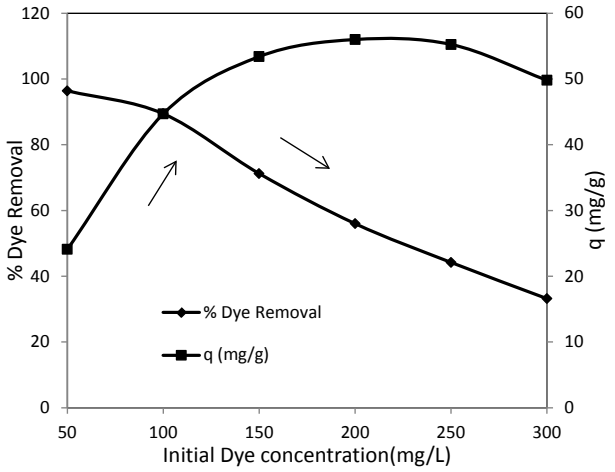

Fig. 12. Effect of initial dye concentration on uptake capacity and percentage dye removal at equilibrium (condition: pH = 6.0, dosage of MPTF = 2 g/L, size of adsorbent = 150 μm, and temperature = 30°C).

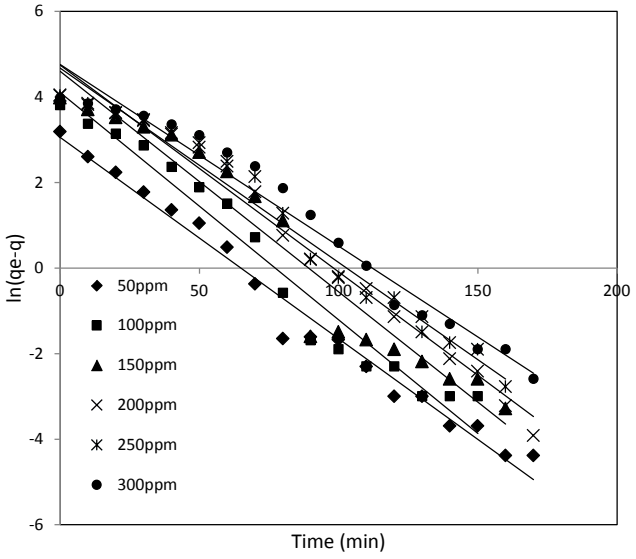

Fig. 13. First-order plots for different initial dye concentrations (condition: pH = 6.0, dosage of MPTF = 2 g/L, size of adsorbent = 150 μm, and temperature = 30°C).

Table 3
List of parameters obtained from pseudo-first-order, pseudo-second-order, Elovich, and intraparticle diffusion for the adsorption of MG onto MPTF

Constants	Initial dye concentrations (mg/L)					
	50	100	150	200	250	300
q_e, experimental (mg/g)	24.3	44.9	53.63	57.22	56.5	53.25
Pseudo-first order						
q_e, calculated (mg/g)	21.18	60.42	99.21	114.58	106.80	116.49
$k_1 \times 10^2$ (min^{-1})	4.71	5.31	5.15	4.83	4.54	4.25
R^2	0.9817	0.9603	0.9391	0.9822	0.9735	0.9702
Ψ^2	0.4596	3.9866	20.9408	28.7150	23.6900	34.3317
Δq_e(%)	8.4457	13.8575	21.7294	23.5990	22.2394	25.6862
Pseudo-second order						
q_e, calculated (mg/g)	26.18	51.02	68.027	75.75	77.52	68.97
$k_2 \times 10^4$ (g/mg min)	14.59	3.84	2.16	1.74	1.66	2.1
R^2	0.9979	0.9927	0.9911	0.9884	0.9931	0.9786
Ψ^2	0.1350	0.7341	3.0469	4.5328	5.6997	3.5830
Δq_e(%)	6.5560	8.7019	12.2123	13.4130	14.3766	12.8065
Elovich						
q_e, calculated (mg/g)	26.03	48.82	58.68	62.83	61.89	58.03
$\alpha \times 10^2$ (mg/g min)	41.0908	5.2392	1.3655	1.036	0.9213	0.5938
β (g/mg)	4.4871	10.608	15.995	17.92	18.185	19.219
R^2	0.8862	0.9001	0.9295	0.929	0.9445	0.9473
Ψ^2	0.1154	0.3155	0.4346	0.5007	0.4698	0.3941
Δq_e(%)	6.2951	6.9684	7.2328	7.3795	7.2815	7.0638
Intraparticle diffusion						
C_1 (mg/g)	0.2402	0.1326	0.4045	0.586	0.6064	0.4331
k_{d1} (mg/g $min^{0.5}$)	0.2108	0.4881	6.7562	7.6244	7.459	7.2903
R_1^2	0.943	0.9721	0.993	0.9901	0.9977	0.9883
C_2 (mg/g)	23.726	44.334	52.731	54.214	53.635	47.67
k_{d2} (mg/g $min^{0.5}$)	0.0444	0.0433	0.0677	0.233	0.2192	0.4337
R_2^2	0.7687	0.9202	0.9818	0.8799	0.8996	0.7456

3.6.3.2. The pseudo-second-order model The kinetic data were further analysed using Ho and McKay's [64] pseudo-second-order kinetics model. This model is based on the assumption that the sorption follows second-order chemisorption. It can be expressed as follows:

$$\frac{t}{q_t} = \frac{1}{k_2 q_e^2} + \frac{t}{q_e} \quad (12)$$

where k_2 is the rate constant. Values of k_2 and q_e were calculated from the plots of t/q_t vs. t in Fig. 14. The k_2, q_e and correlation coefficients R^2 were calculated from this plot and are given in Table 3. From the table, it was observed that the correlation coefficient values for all studied concentrations are higher than 0.99. Also the calculated chi square and Δq_e(%) values are lower, and that suggests that the sorption system could be well described by the pseudo-second-order model. The results from the model recommend the adsorption of MG on MPTF most likely to be controlled by chemisorption process [45,65,66].

3.6.3.3. The Elovich model To describe chemisorption, one of the most useful models is Elovich which is shown in Eq. (13) [67].

$$q_t = \beta \ln \alpha\beta + \beta \ln t \tag{13}$$

where α and β represent Elovich constants, which indicates the initial sorption rate (mg/g min) and the extent of surface coverage and activation energy for chemisorption (g/mg), respectively. The linear plot between q_t and ln$t$ will be used to calculate the parameters α and β from the slope and intercept, as shown in Fig. 15. The estimated Elovich parameters are given in Table 3. The higher R^2 values show that the experimental data are well fitted with the model. Also, the q_e values calculated from Elovich equation agreed quite well with the experimental values which also reflects in low chi-square values. This recommends that the sorption process is controlled by chemisorption process and may involve valence forces between sorbent and sorbate through sharing or exchange of electrons present in the MPTF [68]. Hence, ion exchange mechanism plays a significant role in the sorption process.

3.6.3.4. The intraparticle diffusion model This model was used to find the rate-controlling steps using experimental data which affects the kinetics of adsorption process. Weber's intraparticle diffusion model is shown in Eq. (14) [69].

$$q_t = k_{\mathrm{id}} t^{1/2} + C \tag{14}$$

where C is the intercept and k_{id} is the intra particle diffusion rate constant (mg/g min$^{1/2}$), which can be evaluated from the slope of the linear plot of q_t vs. $t^{(1/2)}$ as shown in Fig. 16. The value of C gives the idea of boundary layer effect on adsorption process. The conditions to be satisfied that the adsorption process obeys intraparticle diffusion are that the plot should be linear and pass through the origin. The deviation of this plot from the linearity indicates that the rate-controlling step should be film diffusion controlled. It was observed from the Fig. 16 that the plots possess multilinear portions (i.e., two steps were involved in the adsorption of MG onto the MPTF). The first and second linear portion indicates film diffusion and intraparticle diffusion, respectively [70–73]. Referring to Fig. 16, the first stage was completed within 90 min for all the dye concentration studied also the linear lines of second stages did not pass through the origin, and this deviation might be due to the difference in the mass transfer rate in the initial and final stages of adsorption [74]. These results prove that the rate-limiting steps in adsorption process are not only by intraparticle diffusion. Rate constant of two stages (k_{d1} and k_{d2}) were found from the slopes of two straight lines and are listed in Table 3. Due to greater driving force, rate constant values are increased with the increasing

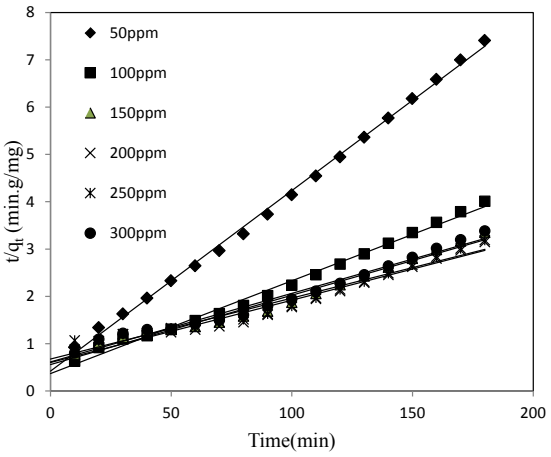

Fig. 14. Second-order plots for different initial dye concentrations (condition: pH = 6.0, dosage of MPTF = 2 g/L, size of adsorbent = 150 μm, and temperature = 30°C).

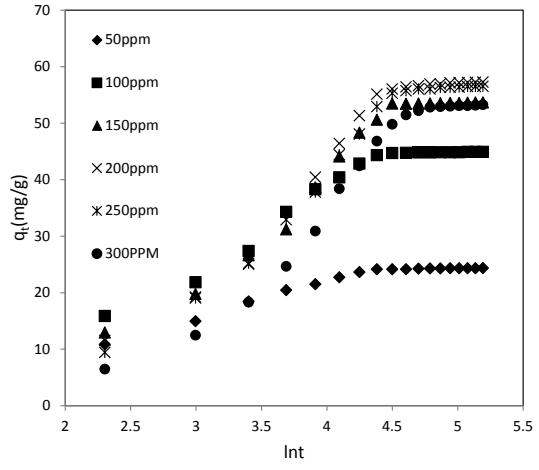

Fig. 15. Elovich plots for different initial dye concentrations (condition: pH = 6.0, dosage of MPTF = 2 g/L, size of adsorbent = 150 μm, and temperature = 30°C).

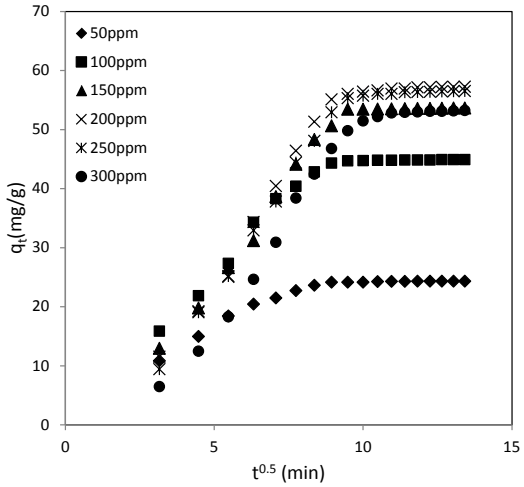

Fig. 16. Intraparticle diffusion plots for different initial dye concentrations (condition: pH = 6.0, dosage of MPTF = 2 g/L, size of adsorbent = 150 μm, and temperature = 30°C).

in initial dye concentration [75]. Consequently from the table, it was observed that the values of k_{d2} are smaller than k_{d1} that confirms that the dye sorption process was controlled by the intraparticle diffusion [76].

3.6.4. Thermodynamic study

From the fundamentals of thermodynamics concepts, for isolated system entropy change is the only driving force [77]. In general, spontaneous natures of the process are identified by using energy and entropy factors. The thermodynamic parameters such as standard Gibbs free energy ($\Delta G°$), enthalpy ($\Delta H°$), and entropy ($\Delta S°$) must be considered to find the spontaneous nature for any adsorption process.

These thermodynamic parameters were evaluated from the following Eqs. (15)–(18).

$$K_c = \frac{C_{Ae}}{C_e} \tag{15}$$

$$\Delta G^\circ = -RT \ln K_c \tag{16}$$

$$\Delta G^\circ = \Delta H^\circ - T\Delta S^\circ \tag{17}$$

$$\ln K_c = \frac{\Delta S^\circ}{R} - \frac{\Delta H^\circ}{RT} \tag{18}$$

where K_c is the equilibrium constant, C_e is the equilibrium concentration in solution (mg/L), and C_{Ae} is the amount of dye adsorbed on the adsorbent per litre of solution at equilibrium (mg/L). R is the gas constant (8.314 J/mol/K) and T is the temperature (K). The values of $\Delta H°$ and $\Delta S°$ are determined from the Van't Hoff equation shown in Eq. (18), and Eq. (17) was used to calculate $\Delta G°$, and the results are listed in Table 4 [78]. Adsorption of MG on MPTF increased when the temperature was increased from 303 to 333 K, and the results are shown in Fig. 17. The plots were used to compute the values of thermodynamic parameters. The negative values of $\Delta G°$ indicate that the process is feasible and spontaneous, and the positive values of $\Delta H°$ indicate that the adsorption process is endothermic nature. The $\Delta S°$ values can be used to describe the randomness at adsorbent–dye solution interface during the sorption [53,79,80].

3.6.5. Comparison of the results with the literature

The Langmuir monolayer adsorption capacity of present adsorption system was compared with the other adsorption system available in literature. The comparison table was shown in Table 5. This comparison was made for the removal of MG dye from aqueous solution by using adsorbents prepared from agricultural waste materials. The results indicated that the maximum adsorption capacity well matches with the other adsorbents.

4. Conclusion

MPTF used in this investigation is easily, abundantly, and locally available and projected to economically feasible for removal of MG from aqueous solution. The adsorption is strongly dependent on initial concentration of dye, pH, adsorbent dosage, and contact time. The removal efficiency increases with increase in pH due to the ionic effect, and an optimum pH value was found to be 6. Also, the removal efficiency increases from 58.2% to 92.6 % for an increase in adsorbent dose from 0.5 to 3 g/L. The increase in initial dye

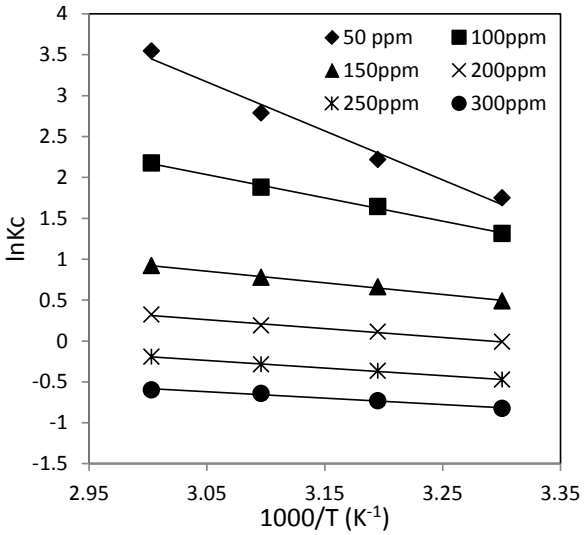

Fig. 17. Van't Hoff plot for different initial dye concentrations (condition: pH = 6.0, dosage of MPTF = 2 g/L, size of adsorbent = 150 μm).

Table 4
Thermodynamic parameters for adsorption of MG onto MPTF at different initial concentrations

Initial dye concentration (mg/L)	$\Delta H°$ (kJ/mol)	$\Delta S°$ (kJ/mol K)	$\Delta G°$ (kJ/mol)			
			303 K	313 K	323 K	333 K
50	49.78506	178.169	–4.20015	–5.98184	–7.76353	–9.54522
100	23.67162	89.10945	–3.32854	–4.21964	–5.11073	–6.00183
150	11.85327	43.24693	–1.25055	–1.68302	–2.11549	–2.54796
200	8.997411	29.61031	–1.025487	–0.27062	–0.56672	–0.86282
250	7.732851	21.60892	–1.04049	–0.82011	–0.59973	–0.37935
300	6.460809	14.53537	–0.66109	–0.47139	–0.28169	–0.09199

Table 5
Comparison of present study with the literature

Name of the adsorbent	q_e (mg g^{-1})	References
Groundnut shell based powdered activated carbon (GSPAC)	222.2	[81]
Tamarind fruit shells activated carbon	83.41	[82]
Rubber seed coat based activated carbon (RSCAC)	72.73	[30]
Activated carbon prepared from male palm tree flower (MPTF)	54.95	Present study
Rice husk activated carbon (RHAC)	49.62	[83]
Activated carbon derived from *Borassus aethiopum* flower biomass (PFAC)	48.48	[32]
Water nut modified carbon (WNMC)	46.27	[31]
Cucumis sativa fruit peel based activated carbon	36.23	[29]
Juglans regia shells based activated carbon	29.74	[84]
Coconut coir activated carbon	27.44	[85]

concentration decreases the percentage dye removal due to the enhanced interaction between MG and MPTF. The percentage dye removal increases with time up to 90 min and no significant increase were observed further. Adsorption isotherms studies show that the adsorption process follows the Langmuir model, and the maximum adsorption capacity was found to be 54.95 mg g^{-1} at 333 k. This was obtained at an optimum condition such as pH 6 and adsorbent dosage 2 g/L. In kinetic analysis, pseudo-second-order kinetic model agrees very well with the dynamic behaviour of the adsorption process. From the thermodynamic analysis, it was concluded that the dye sorption process onto MPTF has endothermic in nature due to the positive value of $\Delta H°$. The positive values of entropy change ($\Delta S°$) show an increase in randomness of the solid–solute interface during the adsorption. Finally, the negative values of $\Delta G°$ indicate the spontaneous nature of the sorption process at the range of temperatures being studied. Because adsorbent used in this study is a waste material which is abundantly and locally available, it is expected to be economically feasible for wastewater treatment.

References

[1] S.V. Awate, N.E. Jacob, S.S. Deshpande, T.R. Gaydhankar, A.A. Belhekar, Synthesis, characterization and photo catalytic degradation of aqueous eosin over Cr containing Ti/MCM-41 and SiO_2-TiO_2 catalysts using visible light, J. Mol. Catal. A. Chem., 226 (2005) 149–154.

[2] A.M.D. Jesus, L.P.C. Romão, B.R. Araújo, A.S. Costa, J.J. Marques, Use of humin as an alternative material for adsorption/desorption of reactive dyes, Desalination, 274 (2011) 13–21.

[3] H.M.H. Mas Rosemal, S. Kathiresan, The removal of methyl red from aqueous solutions using banana pseudostem fibers, Am. J. Appl. Sci., 6 (2009) 1690–1700.

[4] R. Gong, Y. Ding, M. Li, C. Yang, H. Liu, Y. Sun, Utilization of powdered peanut hull as biosorbent for removal of anionic dyes from aqueous solution, Dyes Pigm., 64 (2005) 187–192.

[5] P. Senthil Kumar, S. Ramalingam, C. Senthamarai, M. Niranjanaa, P. Vijayalakshmi, S. Sivanesan, Adsorption of dye from aqueous solution by cashew nut shell: studies on equilibrium isotherm, kinetics and thermodynamics of interactions, Desalination, 261 (2010) 52–60.

[6] C.O. Neill, F.R. Hawkes, D.L. Hawkes, N.D. Lourenço, H.M. Pinheiro, W. Delée, Colour in textile effluents—sources, measurement, discharge consents and simulation: a review, J. Chem. Technol. Biotechnol., 74 (1999) 1009–1018.

[7] P. Nigam, G. Armour, I.M. Banat, D. Singh, R. Marchant, Physical removal of textile dyes from effluents and solid-state fermentation of dye-adsorbed agricultural residues, Bioresour. Technol., 72 (2000) 219–226.

[8] J.R. Easton, The Dye Maker's View in Colour in Dye House Effluent, P. Cooper, Ed., Society of Dyers and Colorists, The Alden Press, Oxford, 1995.

[9] R. Han, D. Ding, Y. Xu, W. Zou, Y. Wang, Y. Li, L. Zou, Use of rice husk for the adsorption of congo red from aqueous solution in column mode, Bioresour. Technol., 99 (2008) 2938–2946.

[10] P.J. Halliday, S. Beszedits, Color removal from textile mill wastewaters, Can. Text. J., 103 (1986) 78.

[11] M. Neamtu, A. Yediler, I. Siminiceanu, M. Macoveanu, A. Kettrup, Decolorization of disperse red 354 azo dye in water by several oxidation processes—a comparative study, Dyes Pigm., 60 (2004) 61–68.

[12] C. Dhandapani, R. Narayanasamy, S.N. Karthick, K.V. Hemalatha, S. Selvam, P. Hemalatha, M. Suresh kumar, S. Dinesh Kirupha, Hee-Je Kim, Drastic photocatalytic degradation of methylene blue dye by neodymium doped zirconium oxide as photocatalyst under visible light irradiation, Optik, 127 (2016) 10288–10296.

[13] K. Kapdan, R. Ozturk, Effect of operating parameters on color and COD removal performance of SBR: sludge age and initial dyestuff concentration, J. Hazard. Mater., B123 (2005) 217–222.

[14] T. Anitha, P. Senthil Kumar, K. Sathish Kumar, Synthesis of nano-sized chitosan blended polyvinyl alcohol for the removal of Eosin Yellow dye from aqueous solution, J. Water Process Eng., 13 (2016) 127–136.

[15] G.S. Gupta, G. Prasad, V.N. Singh, Removal of chrome dye from aqueous solutions by mixed adsorbents: fly ash and coal, Water Res., 24 (1990) 45–50.

[16] R.K. Wahi, W.W. Yu, Y.P. Liu, M.L. Meija, J.C. Falkner, W. Nolte, V.L. Colvin, Photodegradation of Congo Red catalyzed by nanosized TiO_2, J. Mol. Catal. A: Chem., 242 (2005) 48–56.

[17] V.V.B. Rao, S.R.M. Rao, Adsorption studies on treatment of textile dyeing industrial effluent by flyash, Chem. Eng. J., 116 (2006) 77–84.

[18] T. Vidhyadevi, A. Murugesan, S. Dinesh Kirupha, P. Baskaralingam, L. Ravikumar, S. Sivanesan, Adsorption of Congo red dye over pendent chlorobenzylidine rings present on polythioamide resin: kinetic and equilibrium studies, Sep. Sci.Technol., 48 (2013) 1450–1458.

[19] M.B. Amran, M.A. Zulfikar, Removal of Congo red dye by adsorption onto phyrophyllite, Int. J. Environ. Stud., 67 (2010) 911–921.

[20] C. Namasivayam, D. Kavitha, Removal of Congo Red from water by adsorption onto activated carbon prepared from coir pith, an agricultural solid waste, Dyes Pigm., 54 (2002) 47–58.

[21] L. Wang, A. Wang, Adsorption properties of Congo Red from aqueous solution onto surfactant-modified montmorillonite, J. Hazard. Mater., 160 (2008) 173–180.

[22] A.R. Binupriya, M. Sathishkumar, K. Swaminathan, C.S. Ku, S.E. Yun, Comparative studies on removal of Congo red by native and modified mycelial pellets of *Trametes versicolor* in various reactor modes, Bioresour. Technol., 99 (2008) 1080–1088.

[23] C. Smaranda, M. Gavrilescu, D. Bulgariu, Studies on sorption of Congo red from aqueous solution onto soil, Int. J. Environ. Res., 5 (2011) 177–188.
[24] H. Chen, J. Zhao, Adsorption study for removal of Congo red anionic dye using organo-attapulgite, Adsorption, 15 (2009) 381–389.
[25] M.A. Mumin, M.M.R. Khan, K.F. Akhter, M.J. Uddin, Potentiality of open burnt clay as an adsorbent for the removal of Congo red from aqueous solution, Int. J. Enviorn. Sci. Technol., 4 (2007) 525–532.
[26] Z. Zhang, L. Moghaddam, I.M. O'Hara, W.O.S. Doherty, Congo red adsorption by ball-milled sugarcane bagasse, Chem. Eng. J., 178 (2011) 122–128.
[27] M.C.S. Reddy, Removal of direct dye from aqueous solutions with an adsorbent made from tamarind fruit shell, an agricultural solid waste, J. Sci. Ind. Res., 65 (2006) 443–446.
[28] N. Rajamohan, Equilibrium studies on sorption of an anionic dye onto acid activated water hyacinth roots, Afr. J. Environ. Sci. Technol., 3 (2009) 399–404.
[29] T. Santhi, S. Manonmani, Malachite green removal from aqueous solution by the peel of *Cucumis sativa* fruit, Clean Soil Air Water, 39 (2011) 162–170.
[30] M.N. Idris, Z.A. Ahmad, M.A. Ahmad, Adsorption equilibrium of malachite green dye onto rubber seed coat based activated carbon. Int. J. Basic Appl. Sci., 11 (2011) 32–37.
[31] R. Ahmad, P.K. Mondal, Application of modified water nut carbon as a sorbent in congo red and malachite green dye contaminated wastewater remediation, Sep. Sci. Technol., 45 (2010) 394–403.
[32] S. Nethaji, A. Sivasamy, G. Thennarasu, S. Saravanan, Adsorption of malachite green dye onto activated carbon derived from *Borassus aethiopum* flower biomass, J. Hazard. Mater., 181 (2010) 271–280.
[33] K. Geetha, N. Velmani, P.S. Syed Shabudeen, Adsorption efficiency of ceiba pentradenta wood waste onto cationic dye removal, Int. J. Chem. Technol. Res., 8 (2015) 397–410.
[34] D. Balarak, Kinetics, isotherm and thermodynamics studies on bisphenol a adsorption using barley husk, Int. J. Chem. Technol. Res., 9 (2016) 681–690.
[35] P.R. Nirav, U.S. Prapti, K.S. Nisha, Malachite green "a cationic dye" and its removal from aqueous solution by adsorption, Appl. Water Sci., 7 (2017) 3407–3445.
[36] P. Senthil Kumar, A. Saravanan, K. Anish Kumar, R. Yashwanth, S. Visvesh, Removal of toxic zinc from water/wastewater using eucalyptus seeds activated carbon: non-linear regression analysis, IET Nanobiotechnol., 10 (2016) 244–253.
[37] A. Saravanan, P. Senthil Kumar, R. Mugilan, Ultrasonic-assisted activated biomass (fishtail palm *Caryota urens* seeds) for the sequestration of copper ions from wastewater, Res. Chem. Intermed., 42 (2016) 3117–3146.
[38] M. Minamisawa, H. Minamisawa, S. Yoshida, N. Takai, Adsorption behavior of heavy metals on biomaterials, J. Agric. Food Chem., 52 (2004) 5606–5611.
[39] F.A. Pavan, E.C. Lima, S.L.P. Dias, A.C. Mazzocato, Methylene blue biosorption from aqueous solutions by yellow passion fruit waste, J. Hazard. Mater., 150 (2008) 703–712.
[40] M. Srinivas Kini M.B. Saidutta, V. Ramachandra Murty, Studies on biosorption of methylene blue from aqueous solutions by powdered palm tree flower (*Borassus flabellifer*), Int. J. Chem. Eng., 306519 (2014) 1–13.
[41] X.S. Wang, Y. Zhou, Y. Jiang, C. Sun, The removal of basic dyes from aqueous solutions using agricultural by-products, J. Hazard. Mater., 157 (2008) 374–385.
[42] A.A. Jalil, S. Triwahyono, M.R. Yaakob, Utilization of bivalve shell-treated *Zea mays* L. (maize) husk leaf as a low-cost biosorbent for enhanced adsorption of malachite green, Bioresour. Technol., 120 (2012) 218–224.
[43] M.N. Idris, Z.A. Ahmad, M.A. Ahmad, Adsorption equilibrium of malachite green dye onto rubber seed coat based activated carbon, Int. J. Basic Appl. Sci., 11 (2011) 32–37.
[44] C. Namasivayam, D. Prabha, M. Kumutha, Removal of direct red and acid brilliant blue dye by adsorption on to banana pith, Bioresour. Technol., 64 (1998) 77–79.
[45] M.F. Elkady, A.M. Ibrahim, M.M. Abd El-Latif, Assessment of the adsorption kinetics, equilibrium and thermodynamic for the potential removal of reactive red dye using eggshell biocomposite beads, Desalination, 278 (2011) 412–423.
[46] S. Senthilkumaar, P. Kalaamani, C.V. Subburaam, Liquid phase adsorption of crystal violet onto activated carbons derived from male flowers of coconut tree, J. Hazard. Mater., 136 (2006) 800–808.
[47] I. Langmuir, The adsorption of gases on plane surfaces of glass, mica and platinum, J. Am. Chem. Soc., 40 (1918) 1361–1403.
[48] T.W. Weber, R.K. Chakraborty, Pore and solid diffusion models for fixed bed adsorbents, J. Am. Inst. Chem. Eng., 20 (1974) 228–238.
[49] G. Bayramoglu, B. Altintas, M.Y. Arica, Adsorption kinetics and thermodynamic parameters of cationic dyes from aqueous solutions by using a new strong cation-exchange resin, Chem. Eng. J., 152 (2009) 339–346.
[50] R. Sivaraj, C. Namasivayam, K. Kadirvelu, Orange peel as an adsorbent in the removal of acid violet 17 (acid dye) from aqueous solutions, Waste Manage., 21 (2001) 105–110.
[51] H.M.F. Freundlich, Over the adsorption in solution, J. Phys. Chem., 57 (1906) 385–471.
[52] V. Tharaneedhar, P. Senthil Kumar, A. Saravanan, C. Ravikumar, V. Jaikumar, Prediction and interpretation of adsorption parameters for the sequestration of methylene blue dye from aqueous solution using microwave assisted corncob activated carbon, Sustainable. Mater. Technol., 11 (2017) 1–11.
[53] R. Jothirani, P. Senthil Kumar, A. Saravanan, Abishek S. Narayan, Abhishek Dutta, Ultrasonic modified corn pith for the sequestration of dye from aqueous solution, J. Ind. Eng. Chem., 39 (2016) 162–175.
[54] S. Suganya, P. Senthil Kumar, A. Saravanan, P. Sundar Rajan, C. Ravikumar, Computation of adsorption parameters for the removal of dye from wastewater by microwave assisted sawdust: theoretical and experimental analysis, Environ. Toxicol. Pharmacol., 50 (2017) 45–57.
[55] R. Aravindhan, N.N. Fathima, J.R. Rao, B.U. Nair, Equilibrium and thermodynamic studies on the removal of basic black dye using calcium alginate beads, Colloids Surf., A, 299 (2007) 232–238.
[56] M.J. Temkin, V. Pyzhev, Recent modifications to Langmuir isotherms, Acta Physiochim. URSS, 12 (1940) 217–222.
[57] Y. Kim, C. Kim, I. Choi, S. Rengraj, J. Yi, Arsenic removal using mesoporous alumina prepared via a templating method, Environ. Sci. Technol., 38 (2004) 924–931.
[58] P. Waranusantigula, P. Pokethitiyooka, M. Kruatrachuea, E.S. Upatham, Kinetics of basic dye (methylene blue) biosorption by giant duckweed (*Spirodela polyrrhiza*), Environ. Pollut., 125 (2003) 385–392.
[59] M.H. Ehrampoush, G. Ghanizadeh, M.T. Ghaneian, Equilibrium and kinetics study of reactive red 123 dye removal from aqueous solution by asdorption on eggshell, Iran. J. Environ. Health Sci. Eng., 89 (2011) 101–108.
[60] I.D. Mall, S.N. Upadhyay, Studies on treatment of basic dyes bearing wastewater by adsorptive treatment using flyash, Ind. J. Environ. Health, 92 (1998) 177–188.
[61] G. Mckay, Application of surface diffusion model to adsorption of dyes on bagasse pith, Adsorption, 4 (1998) 361–372.
[62] A.A. Inyinbor, F.A. Adekola, G.A. Olatunji, Kinetics, isotherms and thermodynamic modelling of liquid phase adsorption of Rhodamine B dye onto Raphiahookerie fruit epicarp, Water Resour. Ind., 5 (2016) 14–27.
[63] S. Lagergren, B.K. Svenska, Zur theorie der sogenannten adsorption geloester stoffe, Vetenskapsakad. Handl., 24 (1898) 1–39.
[64] Y.S. Ho, G. McKay, Pseudo-second order model for sorption processes, Process Biochem., 34 (1999) 451–465.
[65] F. Banat, A.A. Sameer, A.M. Leema, Utilization of raw and activated date pits for the removal of phenol from aqueous solution, Chem. Eng. Technol., 27 (2004) 80–86.
[66] M. Chairata, R. Saowanee, J.B. Bremnerb, V. Rattanaphani, An adsorption and kinetic study of lac dyeing on silk, Dyes Pigm., 64 (2005) 231–241.

[67] M. Ozacar, I.A. Sengil, A kinetic study of metal complex dye sorption onto pine sawdust, Process. Biochem., 40 (2005) 565–572.
[68] C. Namasivayam, M.V. Sureshkumar, Removal of chromium (VI) from water and wastewater using surfactant modified coconut coir pith as a biosorbent, Bioresour. Technol., 99 (2008) 2218–2225.
[69] A.S. Ozcan, B. Erdem, A. Ozcan, Adsorption of Acid Blue 193 from aqueous solutions onto BTMA-bentonite, Colloids Surf., A, 266 (2005) 73–81.
[70] P. Senthil Kumar, R. Gayathri, C. Senthamarai, M. Priyadharshini, P.S.A. Fernando, R. Srinath, V. Vinoth Kumar, Kinetics, mechanism, isotherm and thermodynamic analysis of adsorption of cadmium ions by surface-modified *Strychnos potatorum* seeds, Korean J. Chem. Eng., 29 (2012) 1752–1760.
[71] P. Senthil Kumar, R.V. Abhinaya, K. Gayathri Lashmi, V. Arthi, R. Pavithra, V. Sathyaselvabala, S. Dinesh Kirupha, S. Sivanesan, Adsorption of methylene blue dye from aqueous solution by agricultural waste: equilibrium, thermodynamics, kinetics, mechanism and process design, Colloid J., 73 (2011) 651–661.
[72] P. Senthil Kumar, R. Sivaranjanee, U. Vinothini, M. Raghavi, K. Rajasekar, K. Ramakrishnan, Adsorption of dye onto raw and surface modified tamarind seeds: isotherms, process design, kinetics and mechanism, Desal. Wat. Treat., 52 (2013) 2620–2633
[73] P. Senthil Kumar, Removal of Congo Red from aqueous solutions by neem saw dust carbon, Colloid J., 72 (2010) 703–709.
[74] K. Mohanty, D. Das, M.N. Biswas, Adsorption of phenol from aqueous solutions using activated carbons prepared from *Tectona grandis* sawdust by $ZnCl_2$ activation, Chem. Eng. J., 115 (2005) 121–131.
[75] A. Ozer, G. Dursun, Removal of methylene blue from aqueous solution by dehydrated wheat bran carbon, J. Hazard. Mater., 146 (2007) 262–269.
[76] M.M. Abd El-Latif, M. Amal Ibrahim, Removal of reactive dye from aqueous solutions by adsorption onto activated carbons prepared from oak sawdust, Desal. Wat. Treat., 20 (2010) 102–113.
[77] K.V. Kumar, A. Kumaran, Removal of methylene blue by mango seed kernel powder, Biochem. Eng. J., 27 (2005) 83–93.
[78] I.A.W. Tan, A.L. Ahmad, B.H. Hameed, Adsorption isotherms, kinetics, thermodynamics and desorption studies of 2, 4, 6-trichlorophenol on oil palm empty fruit bunch-based activated carbon, J. Hazard. Mater., 164 (2009) 473–482.
[79] A. Saravanan, P. Senthil Kumar, C. Femina Carolin, S. Sivanesan, Enhanced adsorption capacity of biomass through ultrasonication for the removal of toxic cadmium ions from aquatic system: temperature influence on isotherms and kinetics, J. Hazard. Toxic Radioact. Waste, 21 (2017) 1–24.
[80] P. Senthil Kumar, Sunita J. Varjani, S. Suganya, Treatment of dye wastewater using an ultrasonic aided nanoparticle stacked activated carbon: kinetic and isotherm modelling, Bioresour. Technol., 250 (2018) 716–722.
[81] R. Malik, D.S. Ramteke, S.R.Wate, Adsorption of malachite green on groundnut shell waste based powdered activated carbon, Waste Manage., 27 (2007) 1129–1138.
[82] A.E. Vasu Studies on the removal of rhodamine B and malachite green from aqueous solutions by activated carbon, J. Chem., 5 (2008) 844–852.
[83] Y.C. Sharma, Adsorption characteristics of a low-cost activated carbon for the reclamation of colored effluents containing malachite green, J. Chem. Eng. Data, 56 (2011) 478–484.
[84] S. Nethaji, A. Sivasamy, A.B. Mandal, Adsorption isotherms, kinetics and mechanism for the adsorption of cationic and anionic dyes onto carbonaceous particles prepared from *Juglans regia* shell biomass, Int. J. Environ. Sci. Technol., 10 (2012) 231–242.
[85] Uma, S. Banerjee, Y.C. Sharma, Equilibrium and kinetic studies for removal of Malachite green from aqueous solution by a low cost activated carbon, J. Ind. Eng. Chem., 19 (2013) 1099–1105.